Experimental observation on a laterally loaded pile in unsaturated silty soil

L.M. Lalicata[1*], A. Desideri[1], F. Casini[2], L. Thorel[3]

[1]*Dipartimento di Ingegneria strutturale e geotecnica. Sapienza Università di Roma. Rome, Italy.*

[2]*Dipartimento di Ingegneria Civile e Ingegneria Informatica, Università` degli Studi di Roma "Tor Vergata", Rome, Italy.*

[3]*IFSTTAR, GERS Department, Geomaterials and Modelling in Geotechnics Laboratory, Bouguenais, France.*

*Corresponding Author: leonardo.lalicata@uniroma1.it

Abstract: An experimental study has been carried out to investigate the effects of soil partial saturation on the behaviour of laterally loaded piles. The proposed study has been conducted by means of centrifuge tests at 100×*g*, where a single vertical pile has been subjected to a combination of static horizontal load and bending moment. The study has been conducted on a silty soil characterized with laboratory testing under saturated and unsaturated conditions. During flight, two different positions of water table have been explored. The influence of density has been investigated compacting the sample with two different void ratio. Finally, the effects of a variation of saturation degree on the pile response under loading have been studied rising the water table to ground surface. Data interpretation allows drawing different considerations on the effects of partial saturation on the behaviour of laterally loaded piles. As expected, compared to saturated soils, partial saturation leads always to a stiffer and resistant response of the system. However, the depth of the maximum bending moment is related to the position of water table and the bounding effects induced by partial saturation appears to be more important for loose soils.

Key words: Centrifuge modelling; unsaturated soils; soil-structure interaction; piles; lateral loading

Introduction

The significant soil volume interested by the kinematics of piles foundation under lateral loading is typically limited vertically in the first meters (several diameters of pile) of depth from ground level. A number of studies available in literature (Banerjee and Davies 1978; Randolph 1981; Krishnan et al. 1983; Higgins et al. 2013, Di Laora and Rovithis 2015) point out that, in this class of problems, the system response is mainly influenced by relative pile soil stiffness ratio, opportunely evaluated in the significant volume of soil, while for short and rigid piles response is affected both by stiffness and slenderness ratio. Most relevant parameters such as head displacement and rotation, maximum bending moment and its position along pile length are also strongly influenced by non-linear stress-strain relationships of soils (Budhu and Davies 1987; Russo 2016).

The behaviour of pile under lateral loading depending, among others factors, from the stiffness of the pile and of the surrounding soil. A flexible (or long) pile is characterized by no variation of load or displacement at the tip level during lateral loading at the head. While, a perfectly rigid (or short) pile should behaves with a constant rotation all along its length. The reality is often in between those idealised two extremes cases.

In many applications, the significant volume of soil can be above the water table, hence in partial saturation conditions. Nowadays, the effects of suction and saturation degree on the mechanical behaviour of soils have been widely investigated

by laboratory studies (Fredlund et al. 1978; Cui and Delage 1996; Escario and Saez, 1986; Vassallo et al. 2007; Casini 2008; Casini et al. 2012; Biglari et al. 2011; Sivakumar and Wheeler 2000; Salager et al. 2013, Hamid and Miller 2009). In the last years, some studies have been published on the influence of partial saturation in engineering problems such us bearing capacity of shallow and deep foundations (Georgiadis et al. 2003; Vanapalli 2009). However, in soil-structure interaction problem, potential benefits of suction are often neglected by practical applications.

Physical centrifuge modelling represents a valid methodology to experimentally investigate soil-structure interaction problems. The small scale model is linked to the full scale prototype, following scaling laws (e.g. Corté 1989; Schofield 1990). When the scale of the model is $1/N$, the model has to be subjected to a centrifuge g-level of N. Studies were so far conducted on fully saturated or completely dried soil model. Only recently, due to a better understanding of the behaviour of compacted soils (Thorel et al. 2011; Caicedo et al. 2014) for the preparation of soil model and to the new instrumentation available to measure suction and saturation degree during the tests (Caicedo and Thorel 2014; Soranzo et al. 2015), unsaturated soil behaviour has been explored by centrifuge modelling (Casini 2008; Thorel et al. 2011; Soranzo et al. 2015). Scaling laws for unsaturated soils have been experimentally investigated by Depountis et al. (2001) and Caicedo et al. (2006). The authors found that capillary rise and diffusion time in the centrifuge could be scaled of $1/N$ and $1/N^2$ respectively. Details of analytical formulation can be found in Caicedo and Thorel (2014) and Soranzo et al. (2015). The scaling factors adopted in this study are listed in Table 1.

The current experimental study is focused on the influence of partial saturation on the behaviour of laterally loaded pile. The aim of the experiment is to study the response of a single vertical free-head pile, embedded in a homogenous fine graded soil, subjected to a combination of lateral loading and bending moment, under different hydraulic condition and initial void ratio. The study has been developed by means of physical modelling in macro-gravity (N=100×g) using the IFSTTAR centrifuge facilities of Nantes (Rosquoët et al. 2007).

The study is organized as follows. First, model and instrumentation set up are reported. Secondly, the soil hydro-mechanical characterization is briefly presented together with the results of flooding test in oedometer apparatus conducted to explore volumetric behaviour during wetting. Thirdly, soil model preparation and test procedures are presented and described. Finally, the results of the study are discussed focusing the attention on the load-head displacement relationship and flexural pile response, exploring the influence of the different structure and soil saturation conditions. In the last section, the effects of a variation of saturation degree on the pile behaviour are analysed.

Experimental facilities

SOIL PROPERTIES

The material used is a commercial kaolin named B-Grade kaolin. The soil has a fine silt fraction of about 90% and a clay fraction of 10%. As reported in Table 2, the material has a liquid limit (w_L) of 42%, a plastic limit (w_P) of 28% and therefore a plastic index (IP) of 14%. The main hydro-mechanical saturated parameters are summarized in Table 2.

In order to define the after compaction conditions (w, e) for centrifuge models, a number of flooding experiments have been performed on samples with different compaction features with a constant vertical stress σ_v=150 kPa. This load corresponds approximately to the vertical stress exerted at half of pile embedded length ($z \cong$ 8m).

Tests are carried out in oedometric apparatus of 70 mm in diameter and 18 mm thick. Following the standard procedure proposed by several authors (Wheeler and Sivakumar 1995; Tarantino and De Col 2008), the soil has been preliminarily dried at 105 °C for 24 hours then demineralized water has been added to reach the desired water content. The material has been kept in sealed bags for 24-48 hours. The specimens have been statically compacted (v=1.5 mm/min) directly in the oedometric ring, allowing to reach quite accurately the required void ratio.

The tests consist of two steps:

- Load at constant water content;
- Soaking at constant load;

The grid of water content and void ratio has been chosen on the base of the results of the Standard Proctor test, black line in Figure 1, from which results an optimum water content (w_{opt}) of 0.21 and an optimum void ratio (e_{opt}) of 0.74 (optimum dry density $\gamma_{d,opt}$=1.528 gr/cm^3). Three voids ratio are taken into account (e_0 = 0.77, 0.92 and 1.12), for water content ranging from 10% to 26%, with steps of 4 %, in order to cover both *dry* than *wet side* of the Proctor curve, Figure 1. For each grid point at least two samples are tested.

Moreover, samples conditions after soaking are presented in Figure 1 with grey symbols, grouped for initial void ratio. All the samples have elevated values of saturation degree, from 0.95 to 1.0. A significant influence of initial void ratio can be recognized: more compacted (e_0=0.77) soil shows a little swelling during wetting while the others exhibit collapse deformation during soaking increasing with initial void ratio. A negligible influence of compaction water content on the deformation upon wetting has been found for this material.

Based on the experimental results obtained, reported in Figure 1, in order to have a collapsible and a swelling soil sample upon wetting, two initial void ratio are selected (0.93 and 0.75) respectively with the same water content w (0.15).

The soil water retention curve (WRC), obtained using the suction controlled oedometric cell (Romero et al. 1995), is presented in Figure 2 in terms of suction and saturation degree relationship. Experimental data refer to the main wetting curve obtained for two different void ratios, 0.93 and 0.75 respectively; both of them has been fitted using Van Genuchten (1980) equation the parameters of which are reported in Table 3. In the suction range experimentally studied, as porosity decrease air entry value ($1/\alpha$) increases from 50 to 166 kPa and the slope of the transition (n) zone reduces from 1.4 to 1.3 in the S_r–s plane. The findings are consistent with literature results (Gens et al. 1995; Romero 1999; Romero and Vaunat 2000; Fredlund and Xing 1994; Tarantino and De Col 2008; Romero et al. 2011). Neglecting for the sake of simplicity the hysteresis of WRC, the as-compacted suction, according to Van Genuchten (1980) equation, is respectively 900 kPa and 3400 kPa for e_0=0.93 (Sr_0=0.43), and e_0=0.75 (Sr_0=0.52).

MODEL AND INSTRUMENTATION

For the purpose of the experiment, 180 mm of soil are statically compacted imposing a constant displacement rate (v=1.5 mm/min), under one-dimensional condition, in a rigid cylindrical container of 300 mm of diameter. A 10 mm thick sand layer, surrounded by geotextile, is laid as drainage layer at the bottom of the model. A 2 mm thick plastic sheet is placed at the border to reduce the container's roughness and shear stresses developing during model preparation. To prevent water evaporation in the upper part of the model, a plastic film covers the soil surface. The bored pile is installed at 1×g, the pre-hole has been realized by means of a manual screwing system of the IFSTTAR facilities (Khemakhem et al. 2010) for an embedded length of 150 mm.

The bottom of the model is connected to a water reservoir the level of which is governed by an electro-pneumatic valves system directly controlled by the operator in the centrifuge control room. A laser sensor measures the water height in the tank.

The model has been extensively instrumented in order to follow both the equalization phases and pile loading, a schematic view of the instrumentation used is proposed in Figure 3. Five LVDT sensors measure soil settlements, two of them are far from the expected interaction zone and they measure the settlements due to flight and consolidation only, the other three are in line with applied load, in the passive area, and can measure also the soil movement during pile loading. The pore water pressure (negative and positive) in the soil is measured with three tensiometers, placed at different depth at the model border. The sensor's range is -500 kPa to 500 kPa. The sensor calibration and saturation procedure of the tensiometer and of the porous stone are described by Mancuso (2011).

The load has been applied at 35 mm from ground level by a hydraulic actuator. The loading phase was displacement-controlled (v=0.003 mm/s at model scale), and a load cell (full scale 2500 N) provided the measure of lateral load. One LVDT built in on a rotational joint gives pile's vertical displacement and rotation.

At the end of each test, undisturbed specimen were sampled all along the model height in order to obtain water content and void ratio distribution with depth.

MODEL PILE CHARACTERISTICS

The 1/100 model pile is a close-ended tube, instrumented with 10 pairs of strain gauges arranged every 15 mm, Figure 4. After a calibration in the lab, the set of gauges deliver the bending moment profile along the pile length. At the prototype scale (N=100×g) the model represents a full circular pile of 1.2 m of diameter, 15 m of embedded length with a bending stiffness of 3.9 GNm^2, subjected to a lateral load applied at 3.5 m from ground surface. The combination of high bending stiffness and relatively small slenderness ratio (L/D = 15/1.2 = 12.5) led to a substantial rigid behaviour of the pile.

Centrifuge test and procedures

MODEL PREPARATION

The soil model used in the centrifuge model has been statically compacted in six layer, with the same procedure followed for the laboratory tests, with w=15% and e_0=0.93 or 0.75 and it is located on *'dry side'* of the Proctor curve. The distribution of vertical compaction stresses, measured during compaction and reported in Figure 5, shows a reasonably good homogeneity for any sample and a very good repeatability of the results in different tests. The compaction stress increases with dry density from a mean value of 500 kPa in the looser state (e_0=0.93) to 1400 kPa in the denser state (e_0=0.75). The homogeneity and repeatability are confirmed also by cone penetration tests (with a diameter of 12 mm) at 1×g reported in Figure 6, referring to low compacted soil. The curves have a similar trend with an increase with depth up to z~50 mm and then are characterized by a mean constant value of q_c~ 3.6 MPa.

EXPERIMENTAL PROGRAMME

On a total of nine tests performed in the centrifuge, four are presented in details, focusing the attention on two parameters: initial void ratio (2 cases) and elevation of the water table (2 cases).

The testing programme is resumed in Table 4 where z_w/L is the water table elevation to embedded length ratio and e_0, w_0, σ_{vc} and Sr_0 are, respectively, the initial void ratio, the gravimetric water content, the compaction stress and the degree of saturation. These values have to be intended as mean values of soil properties.

PROCEDURE

In the main tests (T_06 and T_08) the pile is loaded in unsaturated conditions, until a normalized lateral displacement, y/D, of 30-40% was reached. Then, the water table z_w, has been imposed at 7 m (prototype scale) from ground level. The water table elevation over the embedded length ratio is close to 0.5 (z_w/L = 7/15 = 0.46).

In the following step, the actuator control has been switched from displacement to force control and the water table level has been raised quickly to ground level. The instrumentation on the pile allowed continuous monitoring of head displacement, rotation and bending moments along pile during water table rising.

For the sake of comparison, a pile load has been conducted up to soil failure in fully saturated condition, z_w=0 (T_05 and T_09).

TEST STEPS

The following steps characterize the main tests (T_06, T_08):

1) 1×*g* imbibition: a zero pore pressure is applied at the model base in order to reduce after compaction suction;
2) Flight and application of hydraulic condition at model base: the system has been left in equalization for at least 3 hours;
3) Pile load at displacement control (v=0.003 mm/s);
4) Increase of water table and equalization.

For reference tests in fully saturated condition (T_05 and T_09), only the first three steps are needed; the water table has been directly imposed at ground level.

Results and discussion

In this section are presented selected results to illustrate the influence of soil state condition and partial saturation on the response of laterally loaded piles. The complete results of the experimental program are detailed in Lalicata (2018).

General consideration about soil state at the end of the reference tests on saturated soil for e_0=0.93 (T_05) and e_0=0.75 (T_09) can be deduced by the analysis of the water content and the void ratio distribution with depth reported in Figure 7. Data shows that for e_0=0.93 (T_05) void ratio decreases with depth (typical of soil NC) from a value of ~0.9 at surface to a value of 0.76 for a depth of 17 m; on the other hand, in T_09 (e_0=0.75) the void ratio is mostly constant over the entire range of depth. Moreover, the comparison of the experimental data with the oedometric normal consolidation line, grey line in Figure 7, highlights how the loose soil lays on the NCL below 4 meters of depth, while the denser ones intercept it at 12 meters from ground level. These differences, even for the same stress history prior to pile loading (1×*g* imbibition, increase of total stress and in-flight equalization), may be ascribed both on the different initial void ratio and the different shape of the WRC that controls the variation of mean effective stress and the preconsolidation pressure during hydro-mechanical stress paths (Lalicata 2018).

LATERAL LOAD AT CONSTANT WATER TABLE LEVEL

The load-displacement curves for samples in fully saturated conditions and different void ratio are shown in Figure 8, at the prototype scale. The lateral displacement measurement, y, refers to the displacement at the load application point (nominally 3.5 m above ground level). In the range of lateral displacement explored, the load-displacement relationship is highly non-linear (Rosquoët 2007; Mayne et al. 1995; Russo 2016).

The experimental data can be adequately fitted by means of a hyperbolic function (Mayne et al. 1995):

$$H = \frac{y}{\left(\frac{1}{K} + \frac{1}{H_{\lim}} y\right)} \qquad (1)$$

Where K [MN/m] is the initial stiffness and H_{lim} [MN] is the asymptotic load. In Figure 8, the fitting of hyperbolic function with the load-test data appears to be quite satisfying: dashed and continuous lines are used for e_0=0.75 and 0.93 respectively. The numerical values of lateral stiffness and ultimate load are reported in Table 5.

The strength mobilized, under the applied lateral displacement, is different in asymptotic value and shape for denser and looser samples: for every y value, the H/H_{lim} ratio is higher for e_0=0.93 compared to e_0=0.75. At the end of the test (y=1.6m), for the loose soil (e_0=0.93, T_05) the measured load of 0.7 MN is about the 80% of ultimate capacity H_{lim}. On the contrary, the denser soil, e_0=0.75 (T_09), is still far from the ultimate capacity showing a value of 3.2 MN for the maximum lateral displacement applied (y=1.4 m), giving a load ratio, H/H_{lim}, of 0.55. Initial lateral stiffness increases more than three times as initial void ratio decreases as well. In addition, for low initial void ratio, the load increases almost linearly for a significant displacement range, up to 0.2 m, suggesting that a small amount of yielding occurs in the soil. Furthermore, in the looser state the load-displacement relationship exhibits a non-linear behaviour from low values of displacement, indicating that the soil develops significant plastic strain even for very low load level (Russo and Viggiani 2009). The findings are consistent with the deduced over-consolidation ratio induced by different initial void ratio already commented.

The influence of partial saturation on the load-displacement behaviour is analysed in Figure 9, where the load-displacement curves for looser (Figure 9a) and denser (Figure 9b) samples are reported. In both cases, the partial saturation induces higher stiffness to the soil above the water table, with more appreciable effects for high void ratio. Moreover, for loose soil in presence of partial saturation the load-displacement relationship exhibits an initial linear branch, which cannot be found in saturated condition, consistent with the well-known increment of preconsolidation stress in unsaturated soils (Gens 2010).

It is known that stiffness in fine graded saturated soil depends on mean effective stress p', void ratio e and/or OCR in a non-linear way (Viggiani and Atkinson 1995; Rampello et al. 1994). Most recently other researchers have proposed a

modified formulation to take into account the effect of saturation degree and suction on the small strain stiffness (Biglari et al. 2011), in which stiffness variations are mainly attributed both to the increase of mean effective stress *p'* and to increase the yielding pressure induced by partial saturation (Jommi 2000; Laloui and Nuth 2009; Tamagnini 2004).

Following the generalized effective stress framework (Laloui and Nuth 2009; Bishop and Blight 1963), in unsaturated conditions the main effective stress increases (T_06 and T_08), compared to saturated ones (T_05 and T_09), of the quantity $\Delta p' = \gamma_w \cdot z \cdot (S_r - 1) - \gamma_w \cdot z_w \cdot S_r$. On the other hand, as expected, the stiffness increment due to capillary forces, is better appreciated on the loose soil (e_0=0.93, T_06) which starts from lower values of stiffness. Those increments become less important as the initial structure increases due to the decreasing of initial void ratio.

In addition, the different distribution of saturation degree with depth for the two materials, illustrated in Figure 10, plays an important role in the understanding of the observed behaviour. For sake of simplicity, the plots are evaluated supposing that pore pressures were in hydrostatic conditions ($u = \gamma_w \cdot z_w$); the values of degree of saturation deduced from the SWRC, Table 3, are very different. At ground level, where the differences are more pronounced, the reduction of Sr compared to saturated conditions for the looser soils are 4 times higher than that corresponding to the denser soil. This difference in the distribution of Sr, give an increases in the ratio p'_{cunsat}/p'_{csat} between the preconsolidation pressure in unsaturated conditions p'_{cunsat} and in saturated conditions p'_{csat}, which is properly described with an exponential function of the degree of saturation (e.g. Jommi 2000; Tamagnini 2004; Gallipoli et al. 2003). As well as the stiffness and the strength increases with the decreasing of S_r.

Table 5 summarizes the relative influence of the position of water table, z_w/L, and soil state for lateral stiffness *K* and ultimate load H_{lim} respectively, evaluated by means of eq. (1). Passing from $z_w/L = 0$ to $z_w/L = 0.46$ it can be observed a stiffness increment of more than 300% for high initial void ratio and of 50% low initial void ratio. Therefore, structure effects induced by partial saturation are significantly important for soil with initial open structure because of lower values of saturation degree which allows developing higher bonding effect induced by meniscus. A direct connection between lateral stiffness *K* and soil stiffness E_s cannot be easily recognised because of the pile behaves almost like a rigid pile, hence the head displacement is the sum of a deflection and a rigid rotation (Lalicata 2018) and elastic solutions (Randolph 1981; Higgins et al. 2013; Di Laora and Rovithis 2015) are not directly applicable. In comparison with lateral stiffness, H_{lim} appears to be less affected by partial saturation: compared to saturated condition, gains are 12% for $e_0 = 0.75$ and 220% for $e_0 = 0.93$.

The comparison of bending moment profiles, at 0.1 MN of applied load, for T_08 and T_09 ($e_0 = 0.75$) is presented in Figure 11 (a). The pile does not behaves as a purely flexible pile, since bending moment propagates all along the entire embedded length then the active length of the pile is equal, or even greater of, to the actual length *L* (Randolph 1981). The

stiffness increment in the shallower seven meters from ground level, induced by partial saturation, led to a reduction of maximum bending moment of more than 20% for H=0.1 MN. Thanks to partial saturation, the position of maximum bending moment slightly moves upward passing from 5 to 4 meter from mudline. The small differences of the moment measured at the ground level in the two cases may be ascribed to the different settlement of the soil during the consolidation phase (Lalicata 2018).

Double derivation of moment profile allows calculating the soil pressure distribution along the pile for every load increment. Soil pressure distribution is shown in Figure 11 (b) for the same soil condition and load level of Figure 11 (a). In the shallower part, the unsaturated soil hold higher pressure compared to the saturated one. Pressure remains almost constant in the first 6 meters from ground level and then it reduces smoothly towards the pile tips changing sign at 12 meter of depth.

Referring to almost rigid piles, the findings reported in the present study seems to indicate that the unsaturated zone above water table can change significantly the soil reactions distribution all along the pile length.

The ratio of maximum bending moment obtained for unsaturated condition and saturated condition remains at the constant value of 0.76 for relatively low lateral load, up to 0.5 MN, then it gradually increases to 0.94 measured for H=2.1 MN, as with the increase of the applied load the rigid behaviour becomes dominant compared to the flexural one in both cases (Figure 12).

The bending moment profiles of T_06 and T_08, relative to 0.1 MN of lateral load, are pointed out in Figure 13. This comparison allows to highlight the influence of soil stiffness, here mainly related to initial void ratio and different S_r distribution, on bending response of the pile: as for softer soil (T_06, e_0 = 0.93) the interaction involves greater volumes of soil compared to stiffer ones (T_08, e_0 = 0.75). As expected, the bending moment increases as soil stiffness decreases, and as for the looser sample (T_06), the bending moment distribution is more homogeneous along the entire pile length and the maximum bending moment takes place at greater depth. It is worth noting that all these results are significantly affected by the moment at ground level induced by load eccentricity that significantly increases the values of the maximum bending moment and the downward load transfer (Budhu and Davies 1987).

WATER TABLE RISING AT CONSTANT LOAD

For T_06 and T_08, when the lateral head displacement has reached the 30-40% of the diameter, the loading phase has been stopped and the actuator has been switched from displacement control to loading control. By the electro-pneumatic valves system, the pore pressure at the bottom of the model has been raised quickly from 120 kPa to 190 kPa, in order to simulate the water table raising from 7 m of depth to 0 m. The model has been left in equalization for the remaining time

test (320 min for T_06 and 380 min for T_08, at model scale), the analysis of soil settlements and pore pressure evolution indicates that the stationary condition has not been reached in none of the tests (Lalicata 2018).

Suction decrease, due to imbibition, led to a reduction of mean effective stress and of the preconsolidation pressure (where the collapse for saturation occurs), as well as of the soil stiffness and strength. As a result, the pile head displacement has increased in both tests (Figure 14). Displacement increment resulted higher for open soil structure, T_06, than for closer one, T_08. The global response reported in Figure 14 (a) and (b) is the result of a combination of multiple factors such as differences in saturated permeability, different soil stiffness prior to loading and load ratio level between initial load and ultimate load in saturated condition. First, since saturated permeability decreases with void ratio and, in this phase, the hydraulic equilibrium was far to be reached, lower values of pile lateral displacement are expected for the model with e_0=0.75. Secondly, for the same perturbation applied, higher displacement is expected for loose soil (e_0=0.93) because of lower stiffness. Finally, looking at the comparison between the load-displacement relationship for saturated and unsaturated condition, it seems reasonable to suppose that for e_0=0.93 (Figure 14 (a)) a lateral load of 1.2 MN it is not sustainable in fully saturated conditions; while, for e_0=0.75 even with no suction (Figure 14 (b)), a value of 2.1 MN appears to be sustainable by soil, then the system could have advanced faster to collapse in the first case. However, it is to be noted that the load-deflection curve obtained in saturated conditions (i.e. T_09) not necessarily represents a lower bound solution, given that soil behaviour is strongly nonlinear and dissipative, therefore the final point measured during saturation (grey triangles in Figure 14 (b)) did not represent the end of the process.

The evolution of head displacement with the centrifuge time and the pore pressure for the two tests are presented in Figure 15 (a) and (b). In both Figures, black line refers to e_0=0.93 (T_06), grey colour is used for e_0=0.75 (T_08); in Figure 15 (b) different tensiometers position with depth is illustrated with various style line: a continuous line has been used for z=4m, large dashes for z=9m and, finally, small dashes has been used for z=14m. In order to better emphasize the phenomena, the results are represented in a semi-logarithmic plane and time has been replaced to zero just before the increase of water pressure. Instead of elapsed time, the Terzaghi non-dimensional formulation for time factor has been used: $T = \frac{c_v}{H^2} t$, where c_v is the coefficient of vertical consolidation, t is the elapsed time and H is the drainage layer. For sake of simplicity the same reference values of c_v and H have been adopted for all the tests and are equal to 1.0×10^{-6} m^2/s (Table 2) and 180 mm (initial soil model height) respectively. It is interesting to note that, even if no stabilization occurs, the slope of the pore pressure curves gradually reduces, while the increment of lateral displacement keeps growing; moreover, in the last part of the test, a slight increment of displacement rate can be observed for T_06.

During saturation, the strength reduction in upper part produced the reduction of soil pressure against the pile in the first meters of depth from ground level and an increase in the last meters. Observing the bending moment profiles prior

and post water table rising, it can be observed (Figure 16) a general increment of the moment below the position of the maximum bending moment (from 6 m to 15 m of depth). Since the pile undergoes a rigid body motion during saturation the maximum bending moment variation is less than 10%.

Conclusion

In the present work, the soil pile interaction under lateral loading in unsaturated condition, by means of centrifuge tests has been studied. The models have been statically compacted at two different void ratios and the same water content. The initial conditions have been chosen based on a wide set of flooding tests at different void ratios and water content with the aims to cover a range of void ratios representative of *in situ* soil conditions.

The pile has been loaded with two positions of water table: one at half of pile's embedded length (z_w= 7 m) and the other at ground level (z_w= 0 m). Compared to saturated conditions, a significant increase in lateral stiffness on the load-deflection relationship: 300% for loose soil (e_0=0.93) and 50% for dense soil (e_0=0.75) has been observed in both cases. The effect of partial saturation is stronger for the looser state as, for the same suction, bonding effects due to capillary forces gives a major increment in soil structure. Moreover, the major changes of S_r in the looser sample is given to the different shape of WRC with void ratio.

The present study focus on the behaviour of an almost rigid pile and additional tests are required to investigate the effect of partial saturation varying the soil-pile relative stiffness and the slenderness ratio. In the particular case of rigid pile, that involves a significant volume proportional to the entire embedded length, the increase of soil stiffness in the shallower soil layer leads to a reduction of maximum bending moment more than 20% that moves towards ground surface. For flexible piles that have a critical length lower than the embedded length, the pile response is strongly dependent from the stiffness of the soil close to the surface. Therefore, it is possible that stiffness variation induced by partial saturation may will have more visible effects for flexible piles compared to the rigid pile of this study, which represents a lower bound solution in the understanding of the role of partial saturation in horizontally loaded piles.

During saturation, due to the combination of excessive load level and strong variation of water table level, the system goes towards soil collapse with a close to rigid body motion. Findings appear to show that neglecting the presence of partial saturation is not necessarily a safety solution when significant variation of saturation degree takes place. Reduction of soil strength and stiffness due to saturation can lead to greater pile head displacement than those predicted by fully saturated analysis. The increase of lateral displacement depends both on of the value of the load and the initial water table position.

Acknowledgments

This research has been performed in the framework of the GEO-TRANSALP-PILE-UNSAT agreement developed between DISG, the "Department of Structural and Geotechnical Engineering" of "Sapienza" University of Rome, "Department of Department of Civil and Computer Engineering" University of Rome "Tor Vergata" and IFSTTAR, the "French Institute of Science and Technology for Transport, Development and Networks". They are greatly acknowledged. The authors would like to thank the technical team of the Ifsttar's geo-centrifuge, the technical staff of DISG geotechnical laboratory and also Dr. M. Blanc for his advices.

Notations

Cc	(-)	slope of normalconsolidation line (NCL) in 1D
Cs	(-)	slope of unloading-reloading line (NCL) in 1D
c_v	(m^2/s)	coefficient of vertical consolidation
D	(m)	pile diameter
e	(m)	eccentricity of lateral load
e, e_0, e_{opt}	(-)	void ratio, initial void ratio, optimum void ratio
Es	(MPa)	soil stiffness
g	(m/s^2)	gravitational acceleration
H, H_{lim}	(MN)	lateral load, asympotic lateral load
IP	(%)	plastic index
K	(MN/m)	initial lateral stiffness
k_{sat}	(m/s)	saturated permeability
L	(m)	embedded pile lenght
m	(-)	Van Genuchten parameter
M, M_{sat}	(MNm)	bending moment, maximum bending moment in saturated condition
N	(-)	scaling factor
n	(-)	Van Genuchten parameter
N_0	(-)	reference void ratio on the NCL_1D at σ'_v=1 kPa
OCR	(-)	over consolidation ratio
p'	(kPa)	mean effective stress
q_c	(MPa)	cone resistance of CPT test
s	(kPa)	matrix suction
Sr, Sr_0	(-)	saturation degree, initial saturation degree
Sr_{sat}, Sr_{res}		saturated saturation degree, residual saturation degree
u_w	(kPa)	pore water pressure
v	(mm/s)	compaction rate
v	(mm/s)	lateral displacement rate
w, w_0, w_{opt}	(-)	gravimetric water content, initial gravimetric water content, optimum gravimetric water content
w_L	(%)	liquid limit
w_L	(%)	plastic limit
y	(m)	lateral displacement at the application point
z	(m)	depth
z_w	(m)	water table position
α	(1/kPa)	Van Genuchten parameter
$\gamma_{d,opt}$	(kg/cm^3)	optimum dry density
γ_s	(kN/m^3)	unit weight of solids
γ_w	(kN/m^3)	unit weight of water
φ'	(°)	friction angle

References

Banerjee, P.K., and Davies, T.G. 1978. The behaviour of axially and laterally loaded single piles embedded in nonhomogeneous soils. Géotechnique, **28**(3): 309–326.

Biglari, M., Mancuso, C., d'Onofrio, A., Jafari, M. K., and Shafiee, A. 2011. Modelling the initial shear stiffness of unsaturated soils as a function of the coupled effects of the void ratio and the degree of saturation. Computers and Geotechnics, **38** (5): 709–720. doi:10.1016/j.compgeo.2011.04.007.

Bishop, A., and Blight, G. 1963. Some aspects of effective stress in saturated and partly saturated soils. Géotechnique, **13**(3): 177–197.

Budhu M., and Davies, T.G. 1987. Nonlinear analysis of laterally loaded piles in cohesionless soils. Canadian Geotechnical Journal, **24**(2): 289–296.

Caicedo, B., Medina, C., and Cacique, A. 2006. Validation of time scale factor of expansive soils in centrifuge modeling. *In* Proceedings of the Physical modeling in Geotechnics ICPMG06, Hong Kong, 4-6 August 2006,. Balkema, Rotterdam, pp 273–277.

Caicedo, B., and Thorel, L. 2014. Centrifuge Modelling of Unsaturated soils. Special Issue « Advances in the Mechanics of Unsaturated soils » of the Journal of Geoengineering Sciences, **2**(1-2), 83-103. doi:10.3233/JGS-130013.

Casini, F. 2008. Effetti del grado di saturazione sul comportamento meccanico di un limo. Ph.D. thesis, Department of Structural and Geotechnical Engineering, Sapienza Università di Roma, Rome.

Casini, F., Vaunat, J., Romero, E., and Desideri, A. 2012. Consequences on water retention properties of double-porosity features in a compacted silt. Acta Geotechnica **7**(2): 139–150.

Corté J.F. 1989. Model testing-Geotechnical model tests. *In* Proceedings of the 12th International Conference on Soil Mechanics and Foundation Engineering, XII ICSMFE, Rio de Janerio, 13-18 August 1989. Balkema, Rotterdam, pp 2553-2571.

Cui, Y., and Delage, P. 1996. Yielding and plastic behaviour of an unsaturated compacted silt. Géotechnique, **46**(2): 291–311.

Depountis, N., Davies, M.C.R., Harris, C., Burkhart, S., Thorel, L., Rezzoug, A., Konig, D., Merrifield, C., and Craig, W.H. 2001. Centrifuge modelling of capillary rise. Engineering Geology, **60**(1-4): 95-106.

Di Laora, R., and Rovithis, E. 2015. Kinematic Bending of Fixed-Head Piles in Nonhomogeneous Soil. Journal of Geotechnical and Geoenvironmental Engineering, **141**(4): 04014126. doi: 10.1061/(ASCE)GT.1943-5606.0001270.

Escario, V., and Saez, J. 1986. The shear strength of partly saturated soils. Géotechnique, **36**(3): 453–456.

Fredlund, D.G., and Xing, A. 1994. Equation for the soil-water characteristic curve. Canadian Geotechnical Journal, **31**(4): 521–532.

Gallipoli, D., Gens, A., Sharma, R., and Vaunat, J. 2003. An elasto-plastic model for unsaturated soil incorporating the effects of suction and degree of saturation on mechanical behaviour. Géotechnique, **53**(1): 123–135.

Gens, A. 2010. Soil–environment interactions in geotechnical engineering. Géotechnique, **60**(1): 3–64.

Gens, A., Alonso, E. E., Suriol, J., and Lloret, A. 1995. Effect of structure on the volumetric behaviour of a compacted soil. *In* Proceedings of the first International Conference on Unsaturated Soils, UNSAT '95, Paris, France, 6-8 September 1995. Balkema, Rotterdam, pp 83-88.

Georgiadis, K., Potts, D.M., and Zradvkovic, L. 2003. The influence of partial saturation on pile behavior. Géotechnique, **53**(1): 11–25.

Higgins, W., Vasquez, C., Basu, D., and Griffiths, D.V. 2013. Elastic solution for laterally loaded piles. Journal of Geotechnical and Geoenvironmental Engineering, **139**(7): 1096-1103.

Jommi, C. 2000. Remarks on the constitutive modelling of unsaturated soils. *In* Experimental Evidence and Theoretical Approaches in Unsaturated Soils, Proceedings of the International Workshop on Unsaturated Soils, Trento. Balkema, Rotterdam. pp. 139–153.

Khemakhem, M., Chenaf, N., Garnier, J., Rault, G., Thorel, L., and Dano, C. 2010. Static and cyclic lateral pile behaviour in clay. *In* Proceedings of the 7th International Conference on Physical

Modelling in Geotechnics, ICPMG, 28th June - 1st July 2010, Zurich, Switzerland. Balkema, Rotterdam, pp 953-958.

Krishnan, R., Gazetas, G., and Velez, A. 1983. Static and dynamic lateral deflexion of piles in non – homogeneous soil stratum. Géotechnique, **33**(3): 307 – 325.

Lalicata, L. 2018. Effect of saturation degree on the mechanical behaviour of a single pile subjected to lateral forces (in Italian). Ph.D. thesis, Department of Structural and Geotechnical Engineering, Sapienza Università di Roma, Rome.

Laloui, L., and Nuth, M. 2009. On the use of the generalised effective stress in the constitutive modelling of unsaturated soils. Computer and Geotechnics, **36**(1-2): 20-23. doi:10.1016/j.compgeo.2008.03.002

Mancuso, C., Nicotera, M.V., and Papa, R. 2011. Performances of Two High Capacity Tensiometers. *In* Unsaturated Soils: Research and Applications. 2nd European Conference on Unsaturated Soil. Napoli, 2-4 July. Springer, London, pp 11-17.

Mayne, P.W., Kulhawy, F. H., and Trautmann, C. H. 1995. Laboratory Modeling of Laterally-Loaded Drilled Shafts in Clay. Journal of Geotechnical Engineering, **121**(12): 827-835.

Rampello, S., Silvestri, F. and Viggiani G. 1994b. The dependence of G0 on stress state and history in cohesive soils. *In* Proceedings of the first International Conference on Pre-failure Deformation Characteristics of Geomaterials, Sapporo, Japan,12-14 September 1994. Balkema, Rotterdam, pp 1155-1160.

Randolph, M.F. 1981. The response of flexible piles to lateral loading. Géotechnique, **31**(2): 247–259.

Romero, E. 1999. Characterization and thermo-hydro-mechanical behaviour of unsaturated Boom clay: an experimental study. Ph.D. thesis. Universitat Politecnica de Catalunya Barcelona, Spain.

Romero, E., Della Vecchia, G., and Jommi, C. 2011. An insight into the water retention properties of compacted clayey soils. Géotechnique, **61**(4): 313–328.

Romero, E., Lloret, A., and Gens, A. 1995. Development of a new suction temperature controlled oedometer cell. *In* Proceedings of the first International Conference on Unsaturated Soils, UNSAT '95, Paris, France, 6-8 September 1995. Balkema, Rotterdam, pp 533-539.

Romero, E., and Vaunat, J. 2000. Retention curves of deformable clays. *In* Experimental Evidence and Theoretical Approaches in Unsaturated Soils, Proceedings of the International Workshop on Unsaturated Soils, Trento. Balkema, Rotterdam. pp 90-106.

Rosquoët, F., Thorel, L., Garnier, J., and Canepa, Y. 2007. Lateral cyclic loading of sand-installed piles. Soils and Foundations, **47**(5): 821-832.

Russo, G. 2016. A method to compute the non-linear behaviour of piles under horizontal loading. Soils and Foundation, **56**(1): 33-43.

Russo, G., and Viggiani, C. 2009. Piles under horizontal load: an overview. *In* Foundations: proceedings of the second British Geotechnical Association International Conference on Foundations, ICOF 2008: 24-27 June 2008, University of Dundee, Scotland, UK. Bracknell: IHS BRE Press, pp 61-80.

Salager, S., Nuth, M., Ferrari, A., and Laloui, L. 2013. Investigation into water retention behaviour of deformable soils. Canadian Geotechnical Journal, **50**(2): 200–208.

Schofield, A. N. 1980. Cambridge geotechnical centrifuge operation. Géotechnique **30**(1): 229–267.

Sivakumar, V., and Wheeler, S. J. 2000. Influence of compaction procedure on the mechanical behavior of an unsaturated compacted clay Part 1: Wetting and isotropic compression. Géotechnique, **50**(4): 359–568.

Soranzo, E., Tamagnini, R., and Wu, W. 2015. Face stability of shallow tunnels in partially saturated soil: centrifuge testing and numerical analysis. Géotechnique, **65**(6): 454–467.

Tamagnini, R. 2004. An extended cam-clay model for unsaturated soils with hydraulic hysteresis. Géotechnique, **54**(3): 223–228.

Tarantino, A., and De Col, E. 2008. Compaction behaviour of clay. Géotechnique, **58**(3): 199–213.

Thorel, L., Ferber, V., Caicedo, B., and Khokhar, I. 2011. Physical modelling of wetting-induced collapse in embankment base. Géotechnique, **61** (5), 409–420.

Van Genuchten, M. T. 1980. A closed-form equation for predicting the hydraulic conductivity of unsaturated soils. Soil Science Society of America Journal, **44**(1): 892–898.

Vanapalli, S.K. 2009. Shear strength of unsaturated soils and its applications in geotechnical engineering practice. *In* Unsaturated Soils - Experimental Studies in Unsaturated Soils and Expansive Soils. CRC Press, Newcastle, pp 579-598.

Vassallo, R., Mancuso, C., and Vinale, F. 2007. Effects of net stresses and suction history on the small strain stiffness of a compacted clayey silt. Canadian Geotechnical Journal, **44**(4): 447–462.

Viggiani, G., and Atkinson, J. H. 1995. Stiffness of fine-graded soils at very small strains. Géotechnique, **45** (2): 249-265.

Wheeler, S. J., and Sivakumar, V. 1995. An elasto–plastic critical state framework for unsaturated soil. Geotechnique, **45**(1): 35–53.

Figure Captions

Figure 1: Flooding test results in the compaction plane.

Figure 2: Main wetting Soil Water Retention curves for B-grade Kaolin.

Figure 3: Experimental model: (a) cross section in the load plane, (b) aerial view of the basket, (c) perspective of valve system and soil container, (d) detail of the loading system and LVDT.

Figure 4: Instrumented model pile: (a) schematic cross section, (b) general view.

Figure 5: Vertical compaction stress with depth for different models, each point is located in the middle of one layer.

Figure 6: CPT profiles for e_0=0.93.

Figure 7: Mean values of water content and void ratio with depth after tests T_05 (e_0=0.93) and T_09 (e_0=0.75).

Figure 8: Effect of soil state condition on Lateral Load-Displacement curves (prototype scale).

Figure 9: Load-displacement curves for (a) loose soil (e_0=0.93); (b) dense soil (e_0=0.75).

Figure 10: Different distribution of saturation degree due to different porosity for z_w=7 m.

Figure 11: Influence of water table elevation, z_w =0 (T_09) and z_w =7 m (T_08), for highly compacted soil (e_0=0.75): (a) bending moment distribution along pile, (b) soil reaction distribution along pile.

Figure 12: Maximum bending moment ratio, in unsaturated and saturation condition, for highly compacted soil, e_0=0.75.

Figure 13: Comparison of bending moment distribution along pile for z_w =7 m and different initial void ratio.

Figure 14: Load-displacement curves during saturation for (a) loose soil (e_0=0.93); (b) dense soil (e_0=0.75).

Figure 15: Evolution with time during water table rising of tests T_06 (e_0=0.93) and T_08 (e_0=0.75): (a) lateral displacement, (b) pore pressure at different elevations.

Figure 16: Influence of water table elevation, z_w =0 (T_09) and z_w =7 m (T_08), for highly compacted soil (e_0=0.75): (a) bending moment distribution along pile, (b) soil reaction distribution along pile.

Table 1: Scaling laws for centrifuge modelling.

Parameter	Scaling law model/prototype
Length	1/N
Density	1
Unit weight	N
Stress	1
Strain	1
Force	$1/N^2$
Bending moment	$1/N^3$
Seepage velocity	1/N
Consolidation time	$1/N^2$
Capillary rise	1/N

Table 2: Index properties and hydro-mechanical properties of B-Grade kaolin.

w_L (%)	w_P (%)	IP (%)	ρ_s (gr/cm^3)	C_C (-)	C_S (-)	N_0 (-)	φ' (°)	k_{sat} (m/s)	c_v (m^2/s)
42.2	28.2	14.0	2.66	0.26	0.078	1.36	22	$4.0 \cdot 10^{-9}$	$1.0 \cdot 10^{-6}$

Table 3: Van Genuchten parameters for different void ratio.

e_0 (-)	Sr_{sat} (-)	Sr_{res} (-)	α (1/kPa)	n (-)	m (1-1/n)
0.93	1.0	0.16	0.02	1.4	0.2501
0.75	1.0	0.16	0.006	1.3	0.2307

Table 4: Testing programme.

Name		e_0 (-)	z_w/L (-)	w_0 (%)	σ_{vc} (kPa)	Sr_0 (%)
Test 05	T_05	0.93	0.0	15.03	580	42.02
Test 06	T_06	0.93	0.46	14.67	559	41.01
Test 08	T_08	0.75	0.46	14.72	1395	51.03
Test 09	T_09	0.75	0.0	14.72	1395	51.03

Table 5: Lateral stiffness and asymptotic load.

Test	z_w/L (-)	K (MN/m)	H_{lim} (MN)	e_0 (-)
T_05	0.0	1.5	0.9	0.93
T_06	0.46	6.2	2.9	0.93
T_09	0.0	5.0	5.6	0.75
T_08	0.46	7.4	6.3	0.75

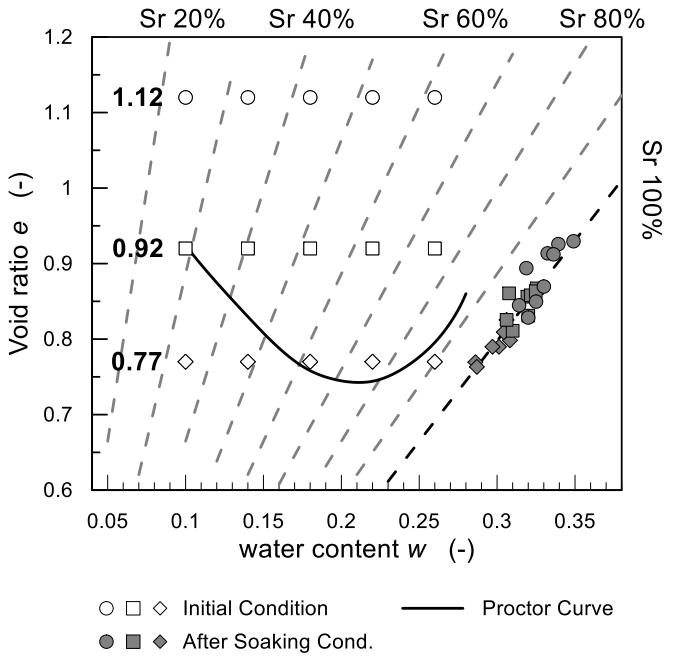

Figure 1: Flooding test results in the compaction plane.

520

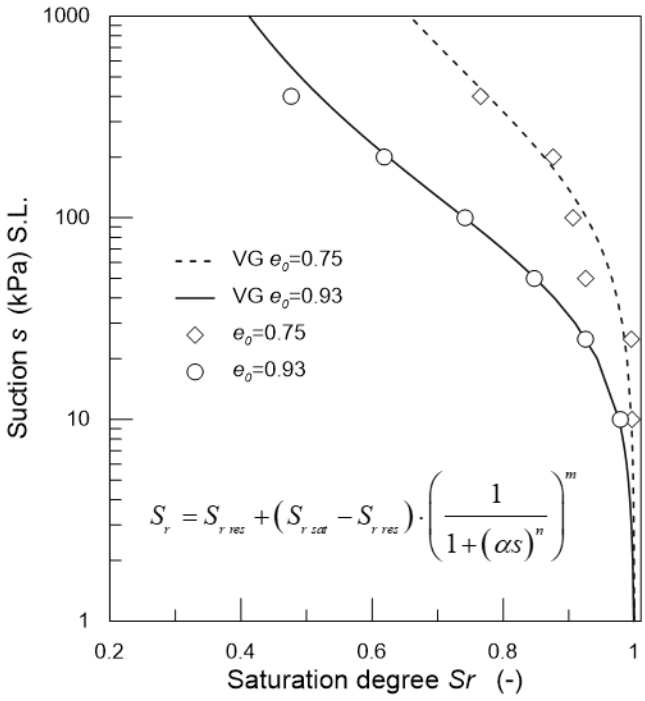

Figure 2: Main wetting Soil Water Retention curves for B-grade Kaolin.

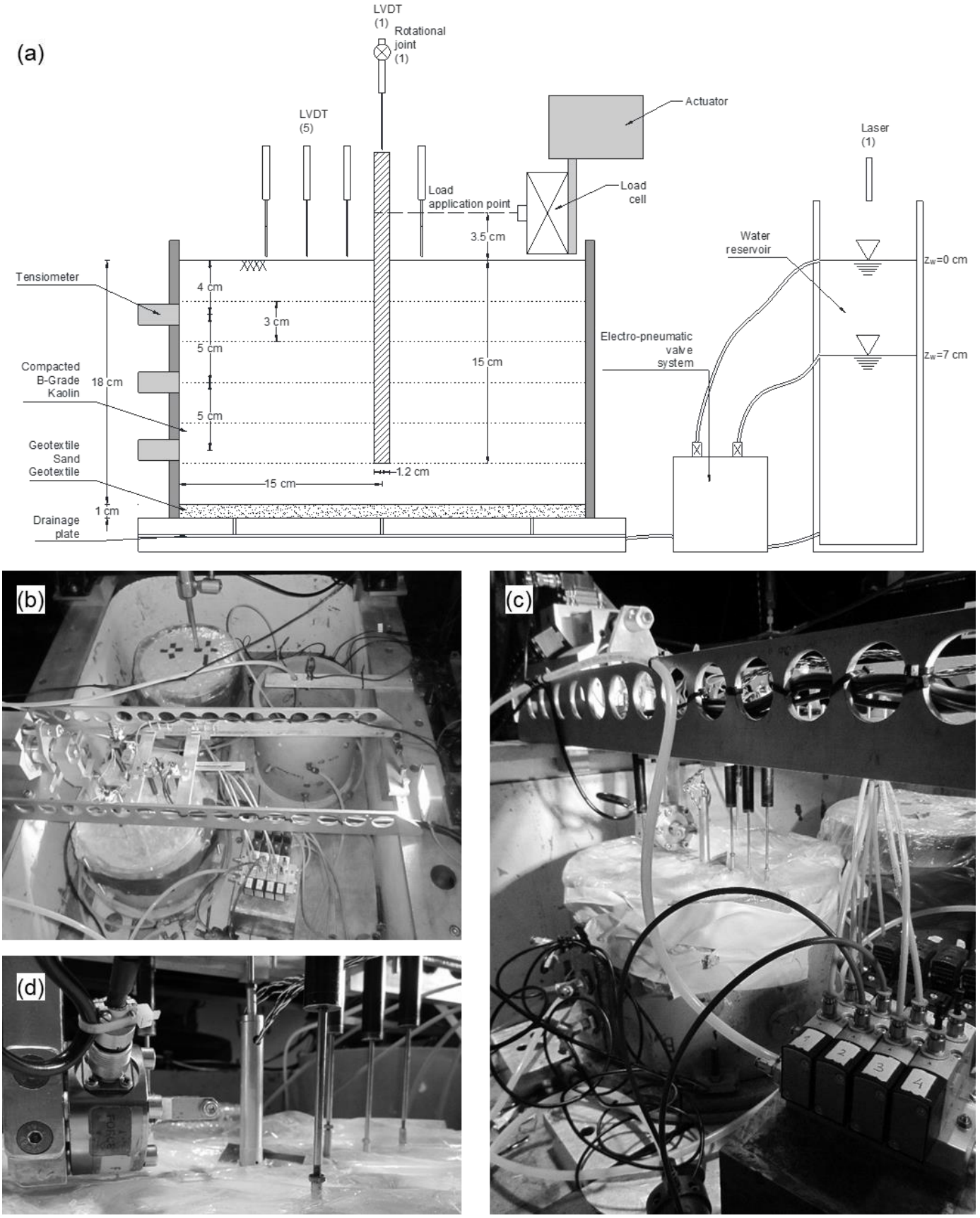

Figure 3: Experimental model: (a) cross section in the load plane, (b) aerial view of the basket, (c) perspective of valve system and soil container, (d) detail of the loading system and LVDT.

526

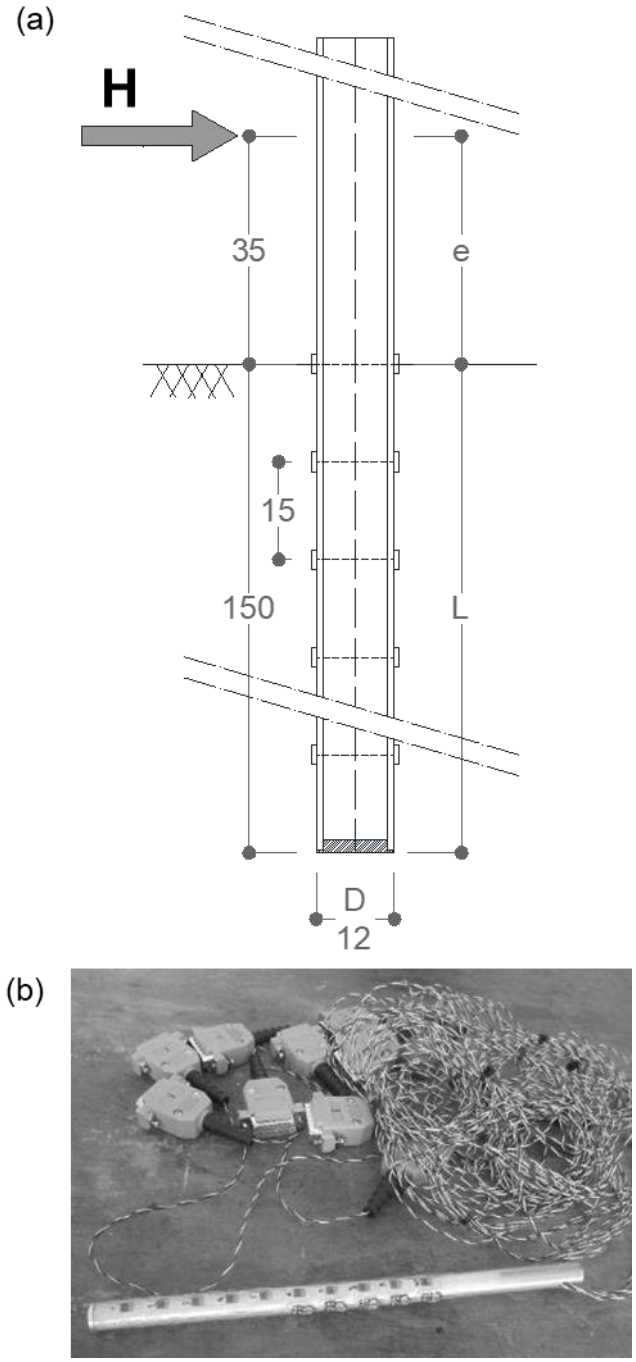

Figure 4: Instrumented model pile: (a) schematic cross section, (b) general view.

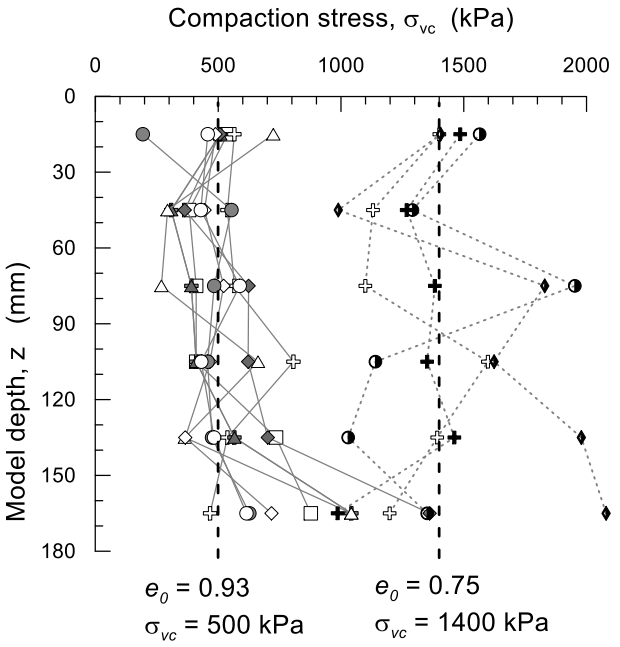

Figure 5: Vertical compaction stress with depth for different models, each point is located in the middle of one layer.

533

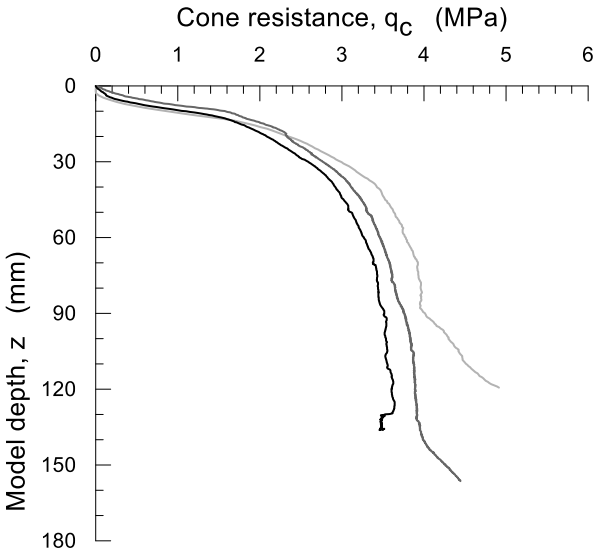

Figure 6: CPT profiles for e_0=0.93.

536

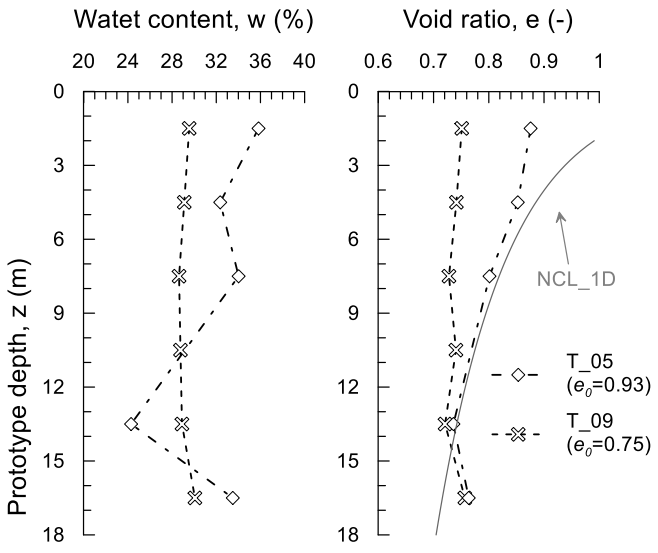

Figure 7: Mean values of water content and void ratio with depth after tests T_05 (e_0=0.93) and T_09 (e_0=0.75).

539

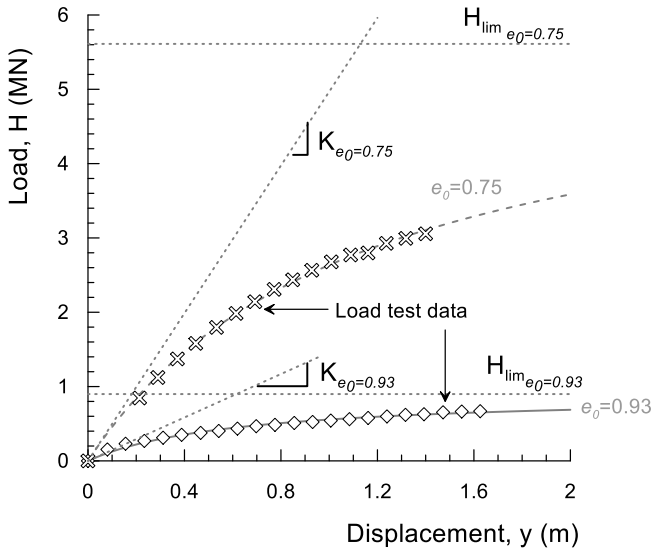

Figure 8: Effect of soil state condition on Lateral Load-Displacement curves (prototype scale).

542

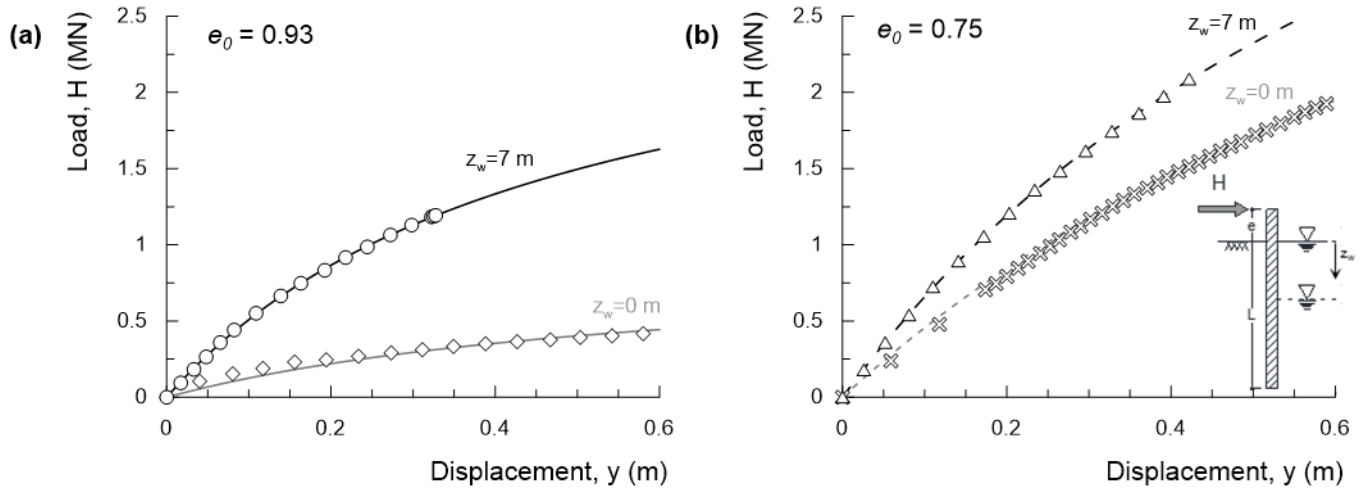

Figure 9: Load-displacement curves: (a) loose soil (e_0=0.93), (b) dense soil (e_0=0.75).

545

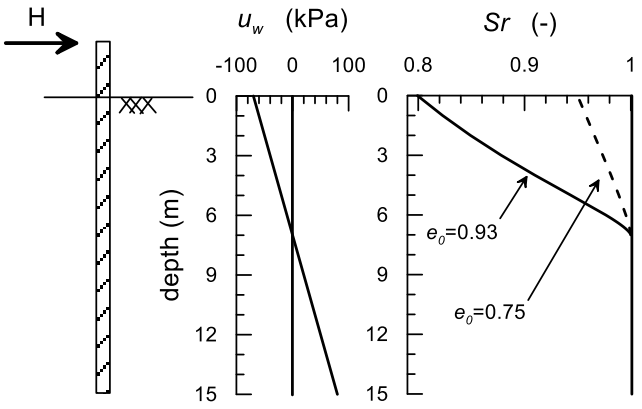

Figure 10: Different distribution of saturation degree due to different porosity for z_w=7 m.

548

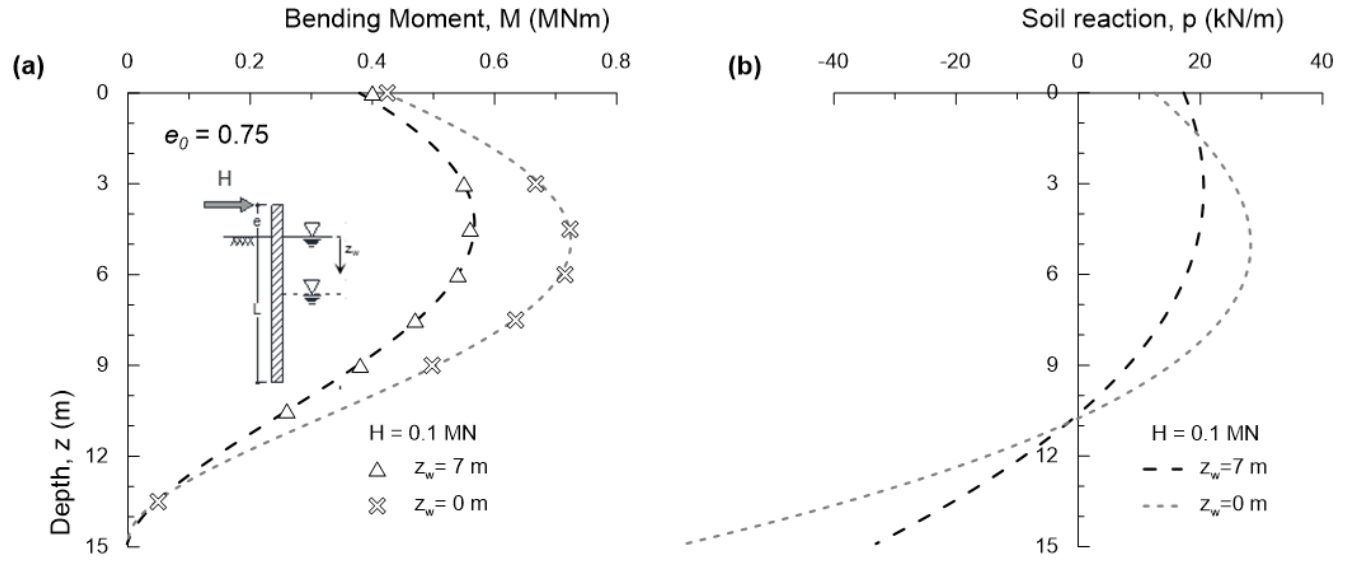

Figure 11: Influence of water table elevation, z_w =0 (T_09) and z_w =7 m (T_08), for highly compacted soil (e_0=0.75): (a) bending moment distribution along pile, (b) soil reaction distribution along pile.

552

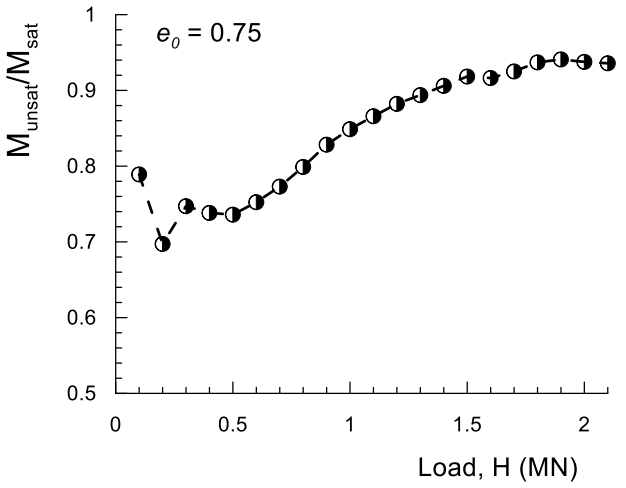

Figure 12: Maximum bending moment ratio, in unsaturated and saturation condition, for highly compacted soil, e_0=0.75.

555

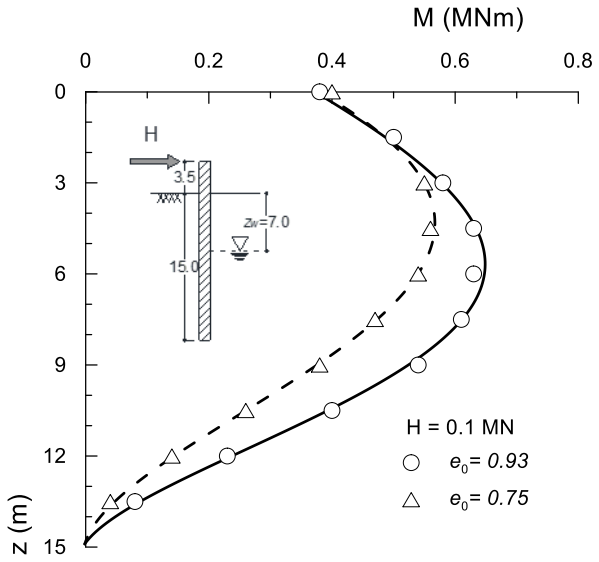

Figure 13: Comparison of bending moment distribution along pile for z_w =7 m and different initial void ratio.

558

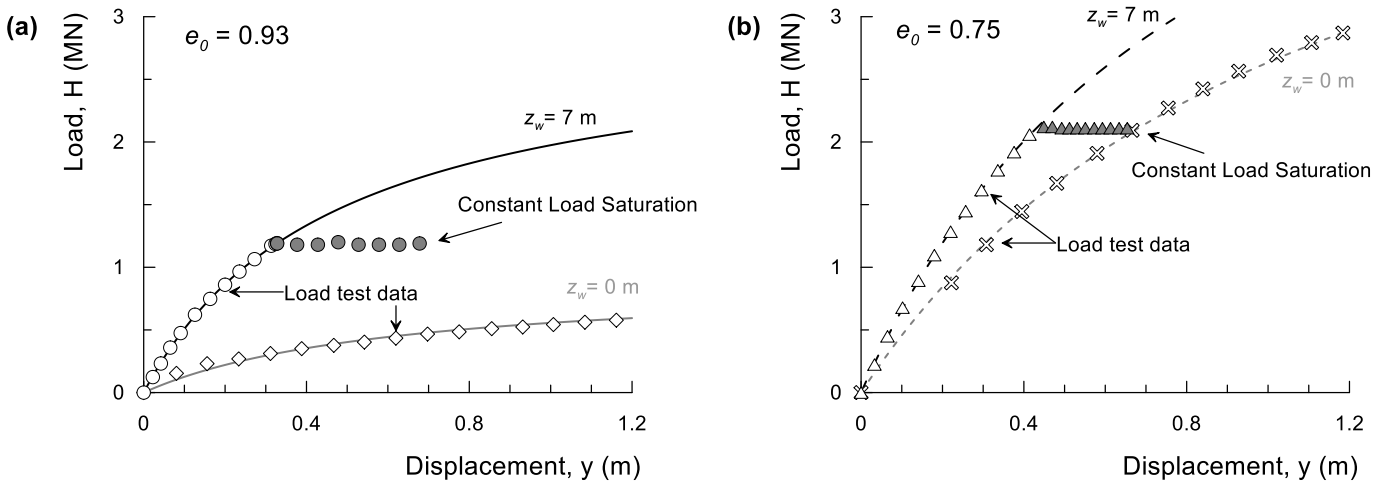

Figure 14: Load-displacement curves during saturation: (a) loose soil (e_0=0.93), (b) dense soil (e_0=0.75).

561

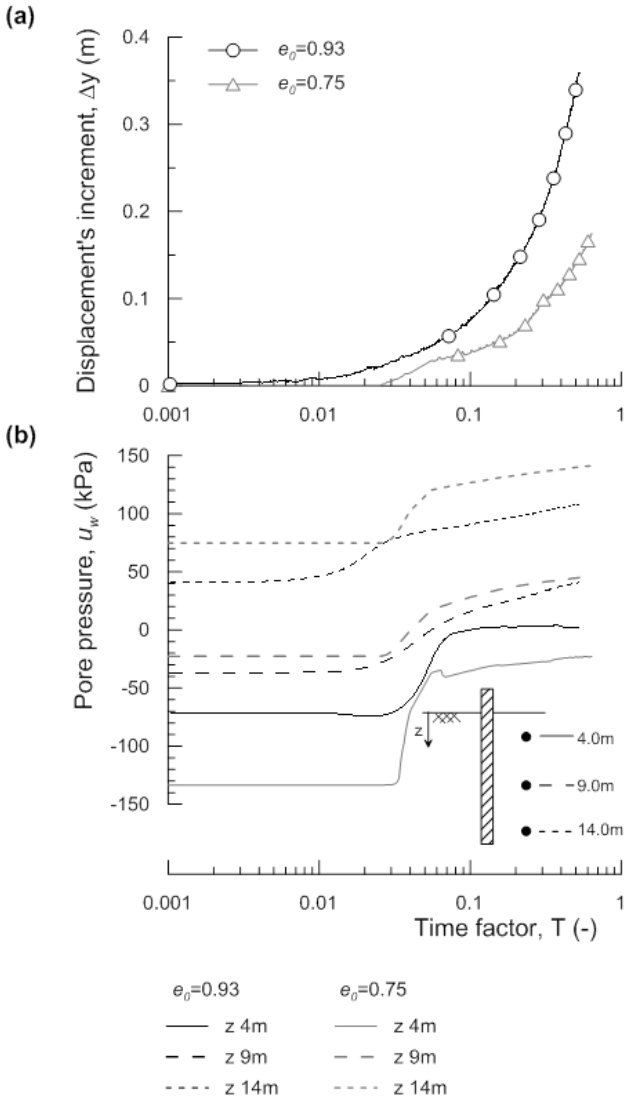

Figure 15: Evolution with time during water table rising of tests T_06 (e_0=0.93) and T_08 (e_0=0.75): (a) lateral displacement, (b) pore pressure at different elevations.

565

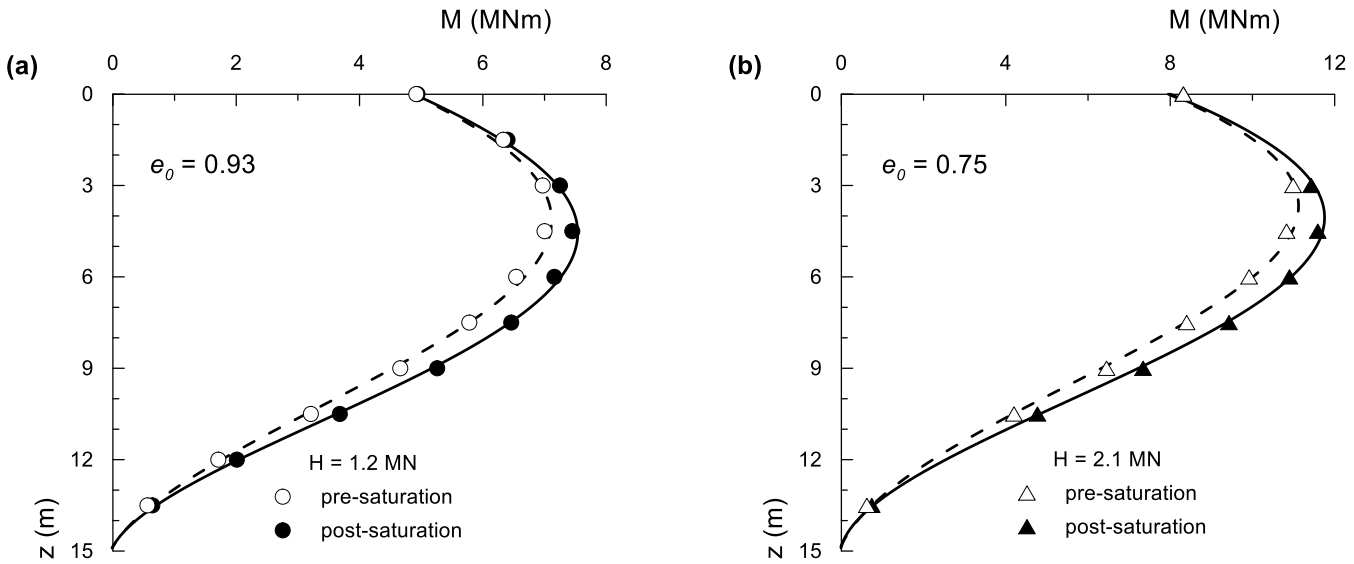

Figure 16: Bending moment profiles before and after saturation: (a) T_06 (e_0=0.93), (b) T_08 (e_0=0.75).